Journal of Zhejiang University-SCIENCE A (Applied Physics & Engineering)
ISSN 1673-565X (Print); ISSN 1862-1775 (Online)
www.jzus.zju.edu.cn; www.springerlink.com
E-mail: jzus@zju.edu.cn

Revisiting aerodynamic admittance functions of bridge decks*

Lin ZHAO[1,2], Xi XIE[1], Teng WU[†‡3], Shao-peng LI[3], Zhi-peng LI[4], Yao-jun GE[1,2], Ahsan KAREEM[5]

[1]*State Key Laboratory of Disaster Reduction in Civil Engineering, Tongji University, Shanghai 200092, China*

[2]*Key Laboratory of Transport Industry of Wind Resistant Technology for Bridge Structures, Tongji University, Shanghai 200092, China*

[3]*Department of Civil, Structural and Environmental Engineering, University at Buffalo, Buffalo, NY 14260, USA*

[4]*School of Civil Engineering, Central South University, Changsha 410000, China*

[5]*Department of Civil & Environmental Engineering & Earth Sciences, University of Notre Dame, Notre Dame, IN 46556, USA*

[†]E-mail: tengwu@buffalo.edu

Received July 25, 2019; Revision accepted Dec. 16, 2019; Crosschecked June 16, 2020

Abstract: A framework was proposed to identify a comprehensive set of aerodynamic admittance functions for bridge decks. The contributions of the cross-spectra between longitudinal and vertical wind velocity components and between turbulence components and gust-induced forces were embedded in the identification procedure. To facilitate application of the identified functions in engineering practice, the concept of an equivalent aerodynamic admittance function was introduced and numerically validated. The equivalent aerodynamic admittance functions of a set of streamlined and bluff cross sections were identified experimentally in a wind tunnel. Buffeting analysis of a bridge deck was carried out and the response predicted using the identified aerodynamic admittance functions compared well with the measured response. In addition, a sensitivity analysis was performed to delineate the influence of aerodynamic and structural parameters on the buffeting response, thereby demonstrating the significance of the proposed identification framework.

Key words: Aerodynamic admittance function; Bridge deck; Buffeting analysis; Wind tunnel test; Sensitivity analysis
https://doi.org/10.1631/jzus.A1900353 **CLC number:** U441.2

1 Introduction

Gust-induced effects on bridges (buffeting), which result in fatigue or serviceability issues, are becoming very important with the increasing span of bridges. Sears' function is the most elementary building block in the linear analysis of gust-induced effects on streamlined bodies in the frequency domain. Liepmann (1952) applied Sears' function to the statistical buffeting analysis of thin airfoils, which was later extended to buffeting analysis of bridges (Davenport, 1962). Davenport (1962) used a linear random vibration-based scheme in which Sears' function was suggested as the aerodynamic admittance function (or based on quasi-steady theory). The aerodynamic admittance function for bluff bodies differs from the Sears' function, and hence needs to be measured in a wind-tunnel (Cao and Sarkar, 2013; Ge and Zhao, 2014). However, due to the complexity involved in wind-tunnel measurements, Sears' function is still employed in the buffeting analysis of bridges.

The identification of the aerodynamic admittance function in a wind tunnel was first carried out by Lamson (1966) for the purpose of verifying Sears' function for a thin airfoil. A systematic experimental identification of the function for bridges (or bluff bodies) surfaced in the 1980s (Walshe and Wyatt, 1983; Jancauskas and Melbourne, 1986). Following this pioneering research, many advanced wind tunnel experimental techniques and identification schemes have recently been proposed to enhance the fidelity of

‡ Corresponding author

* Project supported by the National Natural Science Foundation of China (No. 51778495) and the National Key Research and Development Program of China (No. 2017YFB1201204)

the function. For example, inflow turbulence can be either passively generated by a uniform grid (Sankaran and Jancauskas, 1992; Larose et al., 1998) or actively generated by an array of flaps and airfoils (Diana et al., 2002). The output force generated by the gusts can be measured using the high-frequency balance force technique (Larose and Mann, 1998) or via the surface pressure integral (Sankaran and Jancauskas, 1992). Furthermore, the aerodynamic admittance function can be indirectly identified by measuring the response of a bridge deck model free to oscillate in a wind tunnel considering the incoming turbulences (Gu and Qin, 2004). An alternative approach to obtain the function relies on identified flutter derivatives (Scanlan and Jones, 1999; Hatanaka and Tanaka, 2002; Wu and Kareem, 2014).

To reduce the complexity involved in the experimental identification of the aerodynamic admittance function, several assumptions are usually invoked. In this context, the following concerns need further examination: (1) the spanwise correlation of wind velocity fluctuation in both longitudinal and vertical directions; (2) the relationship between the spanwise correlation of wind fluctuations and gust-induced forces; (3) the contribution from the longitudinal wind fluctuation to the buffeting force; (4) the correlation between the longitudinal and vertical wind fluctuations. There are typically three strategies to consider the spanwise correlation of wind fluctuations, namely reducing the spanwise dimension of the model (Lamson, 1966; Sankaran and Jancauskas, 1992), measuring the spatial correlation of generated turbulence in a wind tunnel (Hatanaka and Tanaka, 2002), and using a 2D aerodynamic admittance function (Larose and Mann, 1998). The spanwise correlation of the buffeting lift force or torsional moment is larger than that of the oncoming turbulence due to "pillow effects", flow separation from the deck, and other underlying mechanisms (Larose, 2003; Haan Jr et al., 2016). However, more research is needed to advance this before the relationship between the spanwise correlations of the incident turbulent fluctuations and the corresponding buffeting forces can be quantitatively determined. Based on quasi-steady theory, it can be inferred that the ratio of contributions from the longitudinal and vertical wind fluctuations to the buffeting forces is proportional to the ratio of the steady-state force coefficients and their derivatives. For a streamlined bridge deck at a small angle of attack, the steady-state coefficient (especially for the lift force and torsional moment) is negligible compared to its derivatives. Hence, it is not unusual for the contribution from the longitudinal fluctuation to be ignored in the experimental identification of the aerodynamic admittance function. When both longitudinal and vertical fluctuations are involved, one would face the difficulty resulting from solving an indeterminate equation (two unknowns in a single equation). One approach to overcome this difficulty is to generate only the longitudinal or vertical fluctuations in the wind tunnel. Uni-directional fluctuations are difficult to generate, hence, it is typically assumed that the aerodynamic admittance functions for the longitudinal and vertical fluctuations are the same (Larose et al., 1998; Gu and Qin, 2004). The correlation between the longitudinal and vertical wind fluctuations is usually ignored, partly due to a lack of cross-spectral data (Nicholas et al., 1998). In multi-mode buffeting analysis, Jain et al. (1996) included the effects of the co-spectra between the longitudinal and vertical wind fluctuations, while the quadratic spectrum was ignored due to a lack of data.

In this study, concerns (3) and (4) mentioned above are further examined. Specifically, a more general identification framework is developed to simultaneously identify a complete set of aerodynamic admittance functions (six in total) considering the contributions of the correlation between the longitudinal and vertical wind fluctuations and of the wind-force correlation between wind fluctuating components and gust-induced forces. To apply the identification results more conveniently to bridge buffeting analysis, an equivalent aerodynamic admittance function is employed, which can encompass concerns (3) and (4) in a simplified way. Note that in all the cases discussed, the nature of the incoming turbulence is assumed not to change along the along-wind direction.

2 Identification of aerodynamic admittance

2.1 Conventional approach

Buffeting forces on a unit-length bridge deck section are conventionally expressed as

$$L_{\mathrm{b}}(t)=\rho UB\cdot\{C_L(\alpha)\chi_{Lu}^{t}u(t)+1/2\left[C_L'(\alpha)+C_D(\alpha)\right]\chi_{Lw}^{t}w(t)\},\tag{1a}$$

$$M_{\mathrm{b}}(t)=\rho UB^2\cdot\left[C_M(\alpha)\chi_{Mu}^{t}u(t)+1/2\,C_M'(\alpha)\chi_{Mw}^{t}w(t)\right],\tag{1b}$$

$$D_{\mathrm{b}}(t)=\rho UB\cdot\{C_D(\alpha)\chi_{Du}^{t}u(t)+1/2\left[C_D'(\alpha)-C_L(\alpha)\right]\chi_{Dw}^{t}w(t)\},\tag{1c}$$

$$S_L(\omega)=\frac{1}{4}\rho^2U^2B^2\cdot\left\{4C_L^2(\alpha)\left|\chi_{Lu}\right|^2S_u(\omega)+\left[C_L'(\alpha)+C_D(\alpha)\right]^2\left|\chi_{Lw}\right|^2S_w(\omega)\right\},\tag{1d}$$

$$S_M(\omega)=\frac{1}{16}\rho^2U^2B^4\cdot\left[4C_M^2(\alpha)\left|\chi_{Mu}\right|^2S_u(\omega)+4C_M^2(\alpha)\left|\chi_{Mu}\right|^2S_u(\omega)\right],\tag{1e}$$

$$S_D(\omega)=\frac{1}{4}\rho^2U^2B^2\cdot\left[4C_D^2(\alpha)\left|\chi_{Du}\right|^2S_u(\omega)+C_D'^{\,2}(\alpha)\left|\chi_{Dw}\right|^2S_w(\omega)\right],\tag{1f}$$

where L_{b}, M_{b}, and D_{b} relate to the lift, torsional, and drag components of the buffeting force, respectively; S is the power spectral density (PSD) function; ρ and U are the air density and inflow mean wind velocity; C and C' represent the steady-state coefficient and the corresponding derivative with respect to the angle of attack α; u and w indicate the longitudinal and vertical components of fluctuating wind velocity, respectively; B is the bridge deck width; t is the time; ω is the natural frequency, $\omega=2\pi n$, and n is the frequency; χ^t is a parameter mapping the wind fluctuations to the gust-induced forces. For example, χ_{Lw}^{t} maps the vertical fluctuating wind to the lift buffeting force. Eqs. (1d), (1e), and (1f) are PSD forms of Eqs. (1a), (1b), and (1c), respectively, in which $|\chi|$ is the modular function of χ^t. It is assumed that wind fluctuations (or buffeting forces) are fully correlated along the deck span. In the frequency domain, the spectrum of a gust-induced lift force is usually expressed as

$$S_{LL}(\omega)=(\rho UB)^2\left|\chi_L(\omega)\right|^2\cdot\{C_L^2(\alpha)S_{uu}(\omega)+1/4\left[C_L'(\alpha)+C_D(\alpha)\right]^2S_{ww}(\omega)\},\tag{2}$$

where $\chi_L(\omega)$ is the aerodynamic admittance function. Typically, Sears' function (or its Liepmann's approximation) is employed in the calculation of buffeting lift force or torsional moment. There are two basic assumptions involved in the use of Eq. (2): (1) $S_{uw}=S_{wu}=0$; (2) $\chi_{Lu}(\omega)=\chi_{Lw}(\omega)=\chi_L(\omega)$.

Fig. 1 shows typical auto-spectra and cross-spectra of the wind velocity fluctuation in full-scale observation and simulation in a wind tunnel (Pan, 2013). Apparently, the absolute value of S_{uw} is not negligible. The contribution to the buffeting response from the relatively small value of the cross-spectrum between the longitudinal and vertical fluctuations needs further examination. Furthermore, the value of the cross-spectrum may become extremely large in the case of wake buffeting.

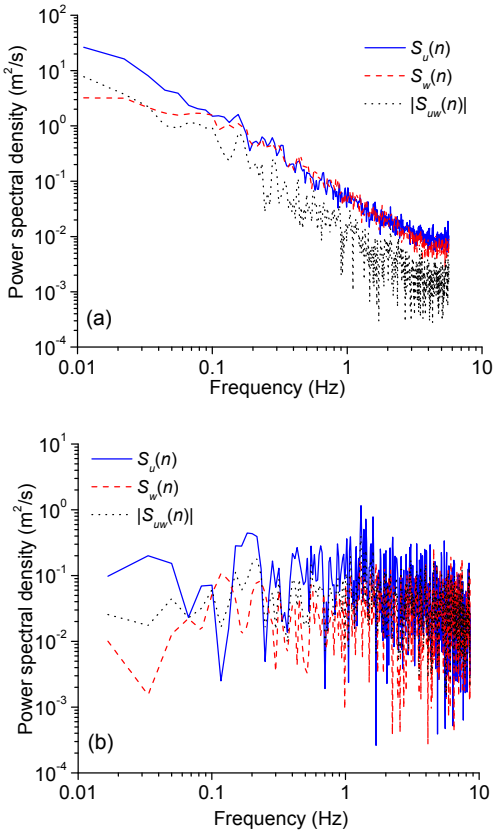

Fig. 1 Auto-spectra and cross-spectra of horizontal and vertical components of fluctuating wind velocity
(a) On-site wind spectra measured at a meteorological station; (b) Wind spectra simulated in a wind tunnel

In the case of a thin airfoil, the relationship between the aerodynamic admittance functions $\chi_{Lu}(\omega)$ and $\chi_{Lw}(\omega)$ can be theoretically derived, and indicates that $\chi_{Lu}(\omega)$ is relatively larger than $\chi_{Lw}(\omega)$

(Horlock, 1968). Assuming the magnitudes of $\chi_{Lu}(\omega)$ and $\chi_{Lw}(\omega)$ are of the same order, based on the observation that C_L is usually much smaller than C_L', especially for streamlined bridge decks, the contribution from longitudinal fluctuation is still negligible. However, this argument may not be valid for the case of bluff bridge decks. Even in the case of streamlined bridge decks, an increase in the wind angle of attack can easily result in an important contribution to the buffeting forces from the longitudinal component of incident wind fluctuation. In addition, the effect of neglecting the contribution of the secondary fluctuation on the buffeting force needs to be assessed. The secondary fluctuation is the longitudinal component of the lift force and torsional moment, and the vertical component of the drag force. Therefore, it may be necessary to identify the full set of six aerodynamic admittance functions for the buffeting analysis of bridge decks.

2.2 Proposed identification scheme

It is not easy to separately generate the u and w fluctuation components in a wind tunnel. Hence, it is more convenient to simultaneously identify the six aerodynamic admittance functions involving the u+w incident turbulent wind. The cross correlation functions between the force component of Eq. (1a) and the longitudinal and vertical wind fluctuations can be expressed respectively as

$$R_{Lu}(\tau)=\rho UB\cdot\{C_L(\alpha)\chi_{Lu}^{t}R_{uu}(\tau)+1/2[C_L'(\alpha)+C_D(\alpha)]\chi_{Lw}^{t}R_{wu}(\tau)\}, \tag{3a}$$

$$R_{Lw}(\tau)=\rho UB\cdot\{C_L(\alpha)\chi_{Lu}^{t}R_{uw}(\tau)+1/2[C_L'(\alpha)+C_D(\alpha)]\chi_{Lw}^{t}R_{ww}(\tau)\}, \tag{3b}$$

where R_{uu} and R_{ww} represent auto-correlation functions of the fluctuating wind velocity components u and w, and R_{wu} and R_{uw} represent the cross-correlation functions, respectively. τ is the time interval. Then, the cross-power spectral density functions are given by

$$S_{Lu}(\omega)=\rho UB\cdot\{C_L(\alpha)\chi_{Lu}(\omega)S_{uu}(\omega)+1/2[C_L'(\alpha)+C_D(\alpha)]\chi_{Lw}(\omega)S_{wu}(\omega)\}, \tag{4a}$$

$$S_{Lw}(\omega)=\rho UB\cdot\{C_L(\alpha)\chi_{Lu}(\omega)S_{uw}(\omega)+1/2[C_L'(\alpha)+C_D(\alpha)]\chi_{Lw}(\omega)S_{ww}(\omega)\}, \tag{4b}$$

where S_{wu} and S_{wu} are the complex cross-power spectra of the turbulent wind velocity components u and w and conjugate each other; S_{Lu} and S_{Lw} are the complex cross-power spectra between the buffeting lift force and the u and w components of fluctuating wind, respectively. From the above equations, the admittance components relating to gust-induced lift force are given by

$$\chi_{Lu}(\omega)=[S_{ww}(\omega)S_{Lu}(\omega)-S_{wu}(\omega)S_{Lw}(\omega)]\cdot\{\rho UBC_L(\alpha)[S_{uu}(\omega)S_{ww}(\omega)-S_{wu}(\omega)S_{uw}(\omega)]\}^{-1}, \tag{5a}$$

$$\chi_{Lw}(\omega)=[S_{uu}(\omega)S_{Lw}(\omega)-S_{uw}(\omega)S_{Lu}(\omega)]\cdot\{1/2\,\rho UB[C_L'(\alpha)+C_D(\alpha)]\cdot[S_{uu}(\omega)S_{ww}(\omega)-S_{uw}(\omega)S_{wu}(\omega)]\}^{-1}. \tag{5b}$$

Similarly, the complex aerodynamic admittance functions for the buffeting torsional moment and drag force are expressed as

$$\chi_{Mu}(\omega)=[S_{ww}(\omega)S_{Mu}(\omega)-S_{wu}(\omega)S_{Mw}(\omega)]\cdot\{\rho UB^2C_M(\alpha)[S_{uu}(\omega)S_{ww}(\omega)-S_{wu}(\omega)S_{uw}(\omega)]\}^{-1}, \tag{6a}$$

$$\chi_{Mw}(\omega)=[S_{uu}(\omega)S_{Mw}(\omega)-S_{uw}(\omega)S_{Mu}(\omega)]\cdot\{1/2\,\rho UB^2C_M'(\alpha)[S_{uu}(\omega)S_{ww}(\omega)-S_{uw}(\omega)S_{wu}(\omega)]\}^{-1}, \tag{6b}$$

$$\chi_{Du}(\omega)=[S_{ww}(\omega)S_{Du}(\omega)-S_{wu}(\omega)S_{Dw}(\omega)]\cdot\{\rho UBC_D(\alpha)[S_{uu}(\omega)S_{ww}(\omega)-S_{wu}(\omega)S_{uw}(\omega)]\}^{-1}, \tag{7a}$$

$$\chi_{Dw}(\omega)=[S_{uu}(\omega)S_{Dw}(\omega)-S_{uw}(\omega)S_{Du}(\omega)]\cdot\{1/2\,\rho UB[C_D'(\alpha)-C_L(\alpha)]\cdot[S_{uu}(\omega)S_{ww}(\omega)-S_{uw}(\omega)S_{wu}(\omega)]\}^{-1}. \tag{7b}$$

To conveniently employ the identified aerodynamic admittance functions in engineering applications,

the equivalent functions for the lift force, torsional moment, and drag force are defined as

$$\begin{aligned}\left|\phi_{LL}(K)\right|^2=&\left\{4C_L^2(\alpha)\left|\chi_{Lu}\right|^2 S_{uu}(K)\right.\\&\left.+\left[C_L'(\alpha)+C_D(\alpha)\right]^2\left|\chi_{Lw}\right|^2 S_{ww}(K)\right\}\\&\cdot\left\{4C_L^2(\alpha)S_{uu}(K)+\left[C_L'(\alpha)+C_D(\alpha)\right]^2 S_{ww}(K)\right\}^{-1},\end{aligned}\tag{8a}$$

$$\begin{aligned}\left|\phi_{MM}(K)\right|^2=&\left[4C_M^2(\alpha)\left|\chi_{Mu}\right|^2 S_{uu}(K)\right.\\&\left.+C_M'^2\left|\chi_{Mw}\right|^2 S_{ww}(K)\right]\\&\cdot\left[4C_M^2(\alpha)S_{uu}(K)+C_M'^2 S_{ww}(K)\right]^{-1},\end{aligned}\tag{8b}$$

$$\begin{aligned}\left|\phi_{DD}(K)\right|^2=&\left\{4C_D^2(\alpha)\left|\chi_{Du}\right|^2 S_{uu}(K)\right.\\&\left.+\left[C_D'(\alpha)-C_L(\alpha)\right]^2\left|\chi_{Dw}\right|^2 S_{ww}(K)\right\}\\&\cdot\left\{4C_D^2(\alpha)S_{uu}(K)+\left[C_D'(\alpha)-C_L(\alpha)\right]^2 S_{ww}(K)\right\}^{-1},\end{aligned}\tag{8c}$$

where $K=\omega B/U$ represents the reduced frequency. Using the equivalent aerodynamic admittance function, the buffeting forces can be calculated with a simple expression similar to Eq. (2) as

$$\begin{aligned}S_{LL}(\omega)=&(\rho UB)^2\left|\phi_{LL}(K)\right|^2\\&\cdot\left\{C_L^2(\alpha)S_{uu}(\omega)+1/4\left[C_L'(\alpha)+C_D(\alpha)\right]^2 S_{ww}(\omega)\right\},\end{aligned}\tag{9a}$$

$$\begin{aligned}S_{MM}(\omega)=&(\rho UB)^2\left|\phi_{MM}(K)\right|^2\\&\cdot\left\{C_M^2(\alpha)S_{uu}(\omega)+1/4\left[C_M'(\alpha)\right]^2 S_{ww}(\omega)\right\},\end{aligned}\tag{9b}$$

$$\begin{aligned}S_{DD}(\omega)=&(\rho UB)^2\left|\phi_{DD}(K)\right|^2\\&\cdot\left\{C_D^2(\alpha)S_{uu}(\omega)+1/4\left[C_D'(\alpha)-C_L(\alpha)\right]^2 S_{ww}(\omega)\right\}.\end{aligned}\tag{9c}$$

2.3 Numerical validation of the equivalent aerodynamic admittance function

Setting $\left|\phi_{\text{Sears}}(\omega)\right|^2 S_{uu}^{\text{tar}}(\omega)$ and $\left|\phi_{\text{Sears}}(\omega)\right|^2 S_{ww}^{\text{tar}}(\omega)$ as target spectra, where ϕ_{Sears} is Liepmann's approximation of Sears' function, we can obtain:

$$\phi_{\text{Sears}}(\omega)=\frac{1}{1+\dfrac{\pi\omega B}{U}}.\tag{10}$$

$S_{uu}^{\text{tar}}(\omega)$ and $S_{ww}^{\text{tar}}(\omega)$ are auto-spectra used in the numerical validation, defined as

$$\frac{nS_{uu}^{\text{tar}}(\omega)}{u_*^2}=\frac{200fu_*^2}{(1+50f)^{5/3}},\tag{11a}$$

$$\frac{nS_{ww}^{\text{tar}}(\omega)}{u_*^2}=\frac{6f}{(1+4f)^2},\tag{11b}$$

where u_* is the Karman friction velocity; f is the non-dimensional quantity $[nz/U(z)]$; z is the height above the ground; $U(z)$ is the mean wind velocity at height z. In addition, the cross-spectrum of u and w is fitted based on the on-site measurement (Fig. 1a) as

$$\left|\frac{nS_{uw}^{\text{tar}}(\omega)}{u_*^2}\right|=\left|\frac{nS_{wu}^{\text{tar}}(\omega)}{u_*^2}\right|=\frac{60fu_*^2}{(1+50f)^{5/3}}.\tag{12}$$

With the above information, the spectral representation scheme (Deodatis, 1996; Chen and Kareem, 2001) can be used to generate the correlated time series of fluctuating wind velocity components $\chi_{Fu}^t u(t)$ and $\chi_{Fw}^t w(t)$ (here, subscript F represents L, M or D, as given in Eqs. (1a), (1b), and (1c)). Based on the aerodynamic parameters of a typical bridge deck section (Table 1), the buffeting force can be simulated time by time through equivalent time-domain transformation of Eqs. (1a), (1b), and (1c) in its PSD type like Eqs. (1d), (1e), and (1f). In this case, the Deodatis ergodic multivariate stochastic simulation algorithm (Deodatis, 1996) can be used for $L_b(t)$ by $S_L(\omega)$. The transformation of buffeting forces from the PSD to time-domain signal can avoid the disturbing issues surrounding the complex quantity of the admittance functions. The aerodynamic admittance functions related to each component of the fluctuating wind velocity can be obtained based on Eqs. (5a) and (5b) for the lift force, Eqs. (6a) and (6b) for the torsional moment, and Eqs. (7a) and (7b) for the drag force. The identification procedure of Eqs. (5)–(8) can be validated by comparing the

obtained equivalent aerodynamic admittance function with ϕ_{Sears} as Eq. (10).

A series of numerical tests were carried out with various characteristics of mean wind velocity (U= 5–10 m/s) and turbulence intensity (I_u=10%–30%, I_w≈0.8I_u) to validate the fidelity of the identification scheme. For promoting engineering applications, the identified equivalent aerodynamic admittance functions are fitted as

$$\lg\left[\phi(\omega)\right]=\sum_{i=0}^{3}\left[\alpha_i\left\{\lg\left(\omega B/U\right)\right\}^i\right], \qquad (13)$$

where α_i is a constant based on least-squares. Compared with a traditional Sears-like monotonically decreasing function, the proposed four-parameter expression is more suitable for complex aerodynamic admittance functions. Fig. 2a shows the identified results (10 simulations) of admittance functions with a mean wind velocity of 10.2 m/s and turbulence intensities of 10.2% (I_u) and 8.1% (I_w). Fig. 2b presents the fitted results based on these 10 simulations. To reduce the variance, the final identification result is obtained by averaging the 10 fitted results. The identification improved as the frequency increased. The accuracy of the identified aerodynamic admittance function in the low-frequency range (reduced frequency less than 0.1) can be improved either by increasing the length of sample data or by improving the fitting scheme. The aerodynamic admittance function in the low frequency range could be approximated using quasi-steady theory, as adopted by Jancauskas and Melbourne (1986). Fig. 3 presents the identification results of five numerical cases with different wind characteristics. The results show that the identified aerodynamic admittance functions were close to the target function (Sears' function), indicating the effectiveness of the identification scheme proposed in this study.

Using the definition of an equivalent aerodynamic admittance function (Eq. (2)) covering the effects of longitudinal $\chi_{Lu}(\omega)$ and vertical components $\chi_{Lw}(\omega)$, respectively, Fig. 4 compares the equivalent admittance and pre-defined Sears' function. Note that the accuracy and feasibility of the proposed algorithm could be validated, and the corresponding equivalent aerodynamic admittance function always remained close to the target function

Table 1 Aerodynamic parameters of a typical streamlined cross section

Parameter	Value
Lift coefficient	0.290
Torsional coefficient	0.012
Drag coefficient	0.134
Lift coefficient derivative	5.026
Torsional coefficient derivative	0.729
Drag coefficient derivative	0.192

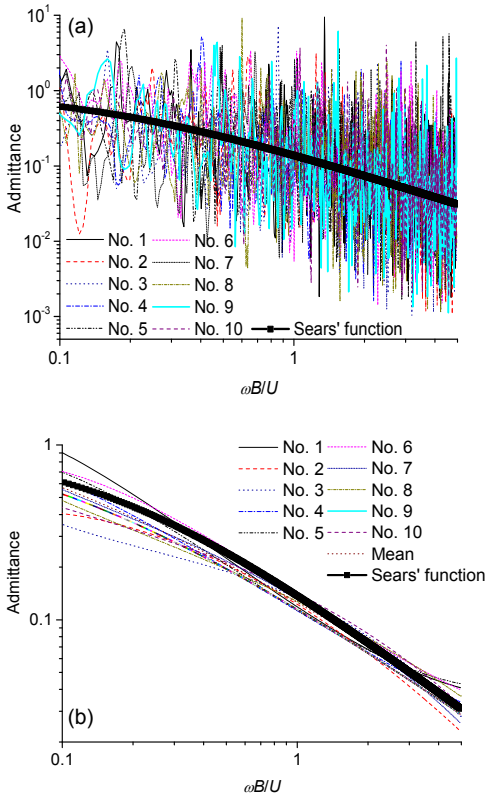

Fig. 2 Identified (a) and fitted (b) results using the proposed identification scheme

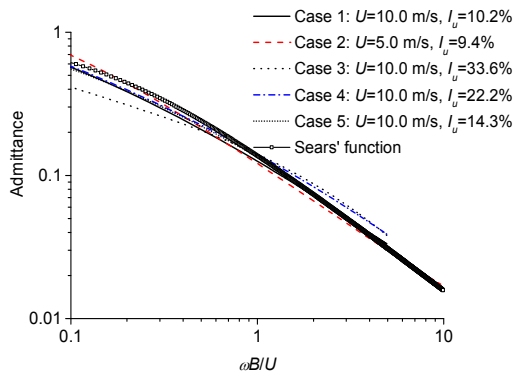

Fig. 3 Identified aerodynamic admittance functions of various cases

(Sears' function). The possible ratio between $|\chi_{Lu}|^2$ and $|\chi_{Lw}|^2$ depends on the cross-spectra of $S_{Lu}(\omega)$, $S_{Lw}(\omega)$, $S_{wu}(\omega)$, and $S_{uw}(\omega)$, as indicated in Eq. (5). For the fitted cross-spectrum given in Eq. (12), the contributions of the longitudinal aerodynamic force $|\chi_L(\omega)|^2 C_L^2(\alpha) S_{uu}(\omega)/S_{LL}(\omega)$ and the vertical aerodynamic force $1/4|\chi_L(\omega)|^2 [C_L'(\alpha)+C_D(\alpha)]^2 \cdot S_{ww}(\omega) \cdot S_{LL}(\omega)^{-1}$ are given in Fig. 5. The contributions of longitudinal and vertical wind fluctuations to the buffeting lift force are nearly the same. On the other hand, if the conventional assumption of $\chi_{Lu}(\omega) = \chi_{Lw}(\omega)$ is employed, the contribution from the longitudinal wind fluctuation will be negligible. For example, with the parameters in Table 1, the contribution from the vertical wind fluctuation is more than 99% of the total lift force.

Using the equivalent aerodynamic admittance function, the buffeting forces can be calculated using a simple expression similar to Eq. (2).

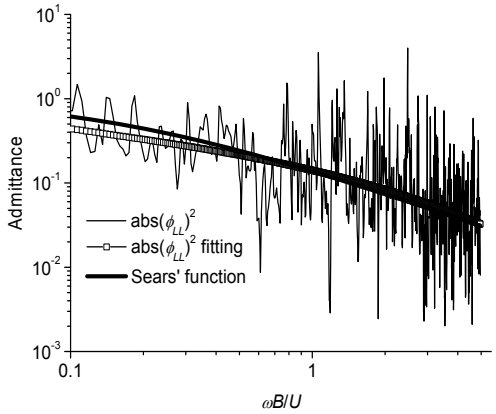

Fig. 4 Equivalent aerodynamic admittance covering longitudinal and vertical components

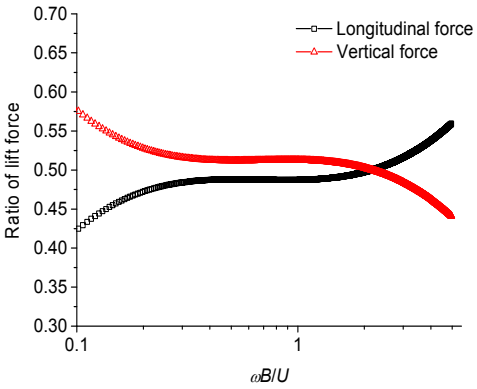

Fig. 5 Contributions of longitudinal and vertical wind fluctuations to buffeting lift force

3 Aerodynamic admittance identification of a streamlined bridge deck in a wind tunnel

3.1 Wind tunnel setup

Experiments were conducted in the TJ-1 Boundary Layer Wind Tunnel of Tongji University with a test section of 1.2 m wide, 1.8 m high, and 18.0 m long. A typical streamlined bridge deck was used in the experimental test (Fig. 6). The model was made of light and thin-walled wood with the desired rigidity. The streamlined box section model comprised a measurement segment (30 cm long) and dummy segments 30 cm and 15 cm high above and below, respectively (Fig. 7). The length of the measurement segment was comparable to the integral scale of the incident turbulence. Hence, the spanwise wind velocity fluctuations (and the buffeting forces) were assumed to be fully correlated. The force measuring equipment was a bottom-supported five-component strain-gauge balance. A customized three-component high-frequency force balance was used. The maximal measurement ranges for shear force and torsional moment were 20 N and 2 N·m with sensitivity indexes of 2g and 20g·cm, respectively, and the precision was about 1‰–2‰ of the measurement range. The natural frequency of the force measuring system

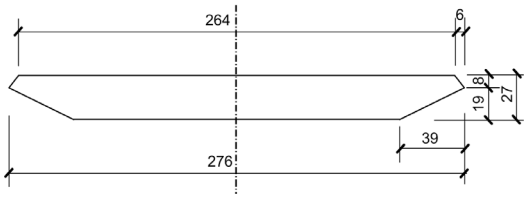

Fig. 6 Cross section of a typical streamlined bridge deck used in the identification of aerodynamic admittance (unit: mm)

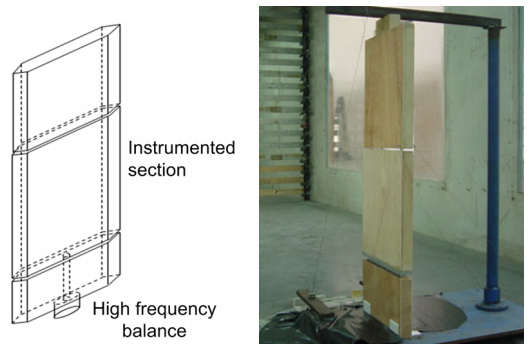

Fig. 7 Arrangement of the sectional model in the wind tunnel

was much higher than the frequency of interest relevant to the dynamic values of the bridge system, which was larger than the measurement frequency band of buffeting aerodynamics.

The steady-state coefficients of the streamlined bridge deck were measured in a uniform flow with a wind angle of attack at 0° (Table 1). Four turbulence flow fields were simulated using passive grids (Table 2), in which L_u^x and L_w^x are the longitudinal and vertical turbulence integrals, respectively. Dantec streamline hotline anemometers made in Denmark were used to measure the oncoming fluctuating wind velocity. The effective measuring range was 0.02–60.0 m/s with a precision of 1.5‰. In the wind tunnel, the turbulence integral varied slightly from the listed values for various flow intensities (Table 2).

3.2 Aerodynamic admittance identification

Fig. 8 presents the identified equivalent admittance function with wind characteristics of U=

Table 2 Turbulence parameters

No.	U (m/s)	L_u^x (cm)	L_w^x (cm)	I_u (%)	I_w (%)
1	4.0–10.0	28±4.2	15±2.5	11.5±1.2	6.5±0.4
2				19.8±1.7	13.9±2.6
3				26.8±2.4	14.9±2.9
4				30.0±3.4	17.2±3.2

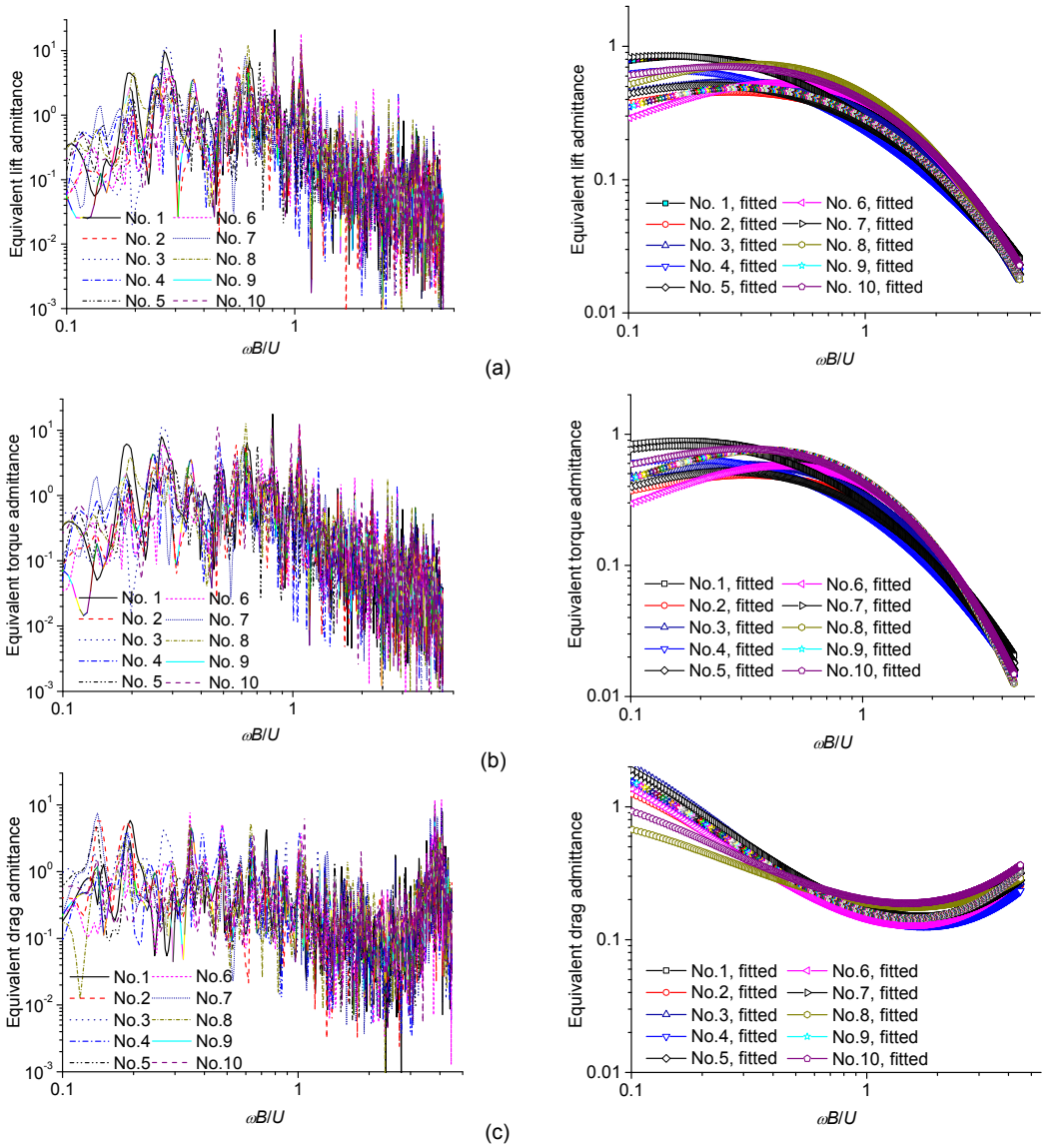

Fig. 8 Identified equivalent aerodynamic admittance functions (left) and their fitting curves (right)
(a) Lift force; (b) Torsional moment; (c) Drag force

9.62 m/s, I_u=11.5%, and I_w=6.5%, and compares the results of discrete point graphs and fitting graphs. A set of ten experimental tests showed that the fitted results based on Eq. (13) were relatively consistent.

Note that the obtained equivalent aerodynamic admittance functions based on the proposed identification scheme were compared to those based on the stochastic subspace identification technique (SSIT), which has been shown to be an effective approach to obtain the aerodynamic admittance (Gu and Qin, 2004). Some discrepancies between the results from the two schemes (Fig. 9) could be attributed to system identification error and to the assumption of $\chi_{Fu}(\omega)=\chi_{Fw}(\omega)$ adopted by Gu and Qin (2004).

Fig. 10 presents the identified equivalent aerodynamic admittance functions for various levels of turbulence intensity. The results suggest that a large variance in the functions is associated with different incident wind characteristics, and no obvious trend was observed. This variance may be attributed to a number of sources, especially the condition of high incoming turbulence intensities, the spanwise correlation of wind fluctuation and buffeting force (Xu et al., 2014), integral scale (Larose and Mann, 1998), secondary flow due to the separation (Matsuda et al., 1999), Reynolds number effects (Matsuda et al., 2001), and aerodynamic nonlinearity (Ma et al., 2013). Since the admittance theoretical framework has been proposed based largely on the analytical Sears' function, it is widely used to modify the non-steady effect between incoming turbulence and aerodynamic loading around a streamlined body. However, the analytical solution of Sears' function is based on an important assumption that means it is suitable only for a 2D airfoil cross section under non-vortex potential flow, and only sinusoidal vibration of the airfoil is taken into account to obtain the equivalent 2D incoming wind wave. Once 3D

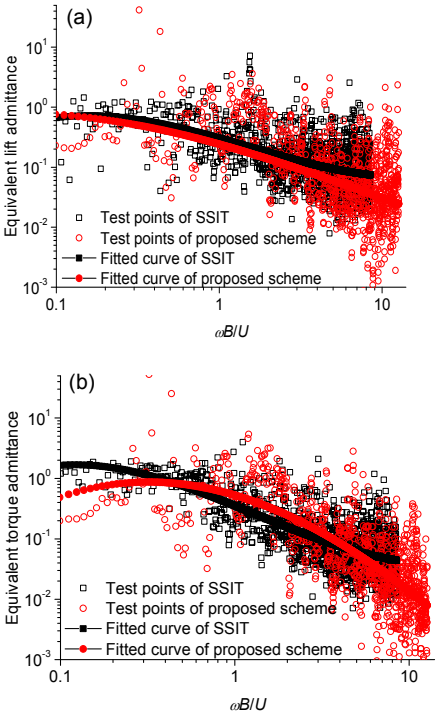

Fig. 9 Comparison of aerodynamic admittance functions based on two different identification schemes (U=5.3 m/s and I_u=11.5%): (a) lift force; (b) torsional moment

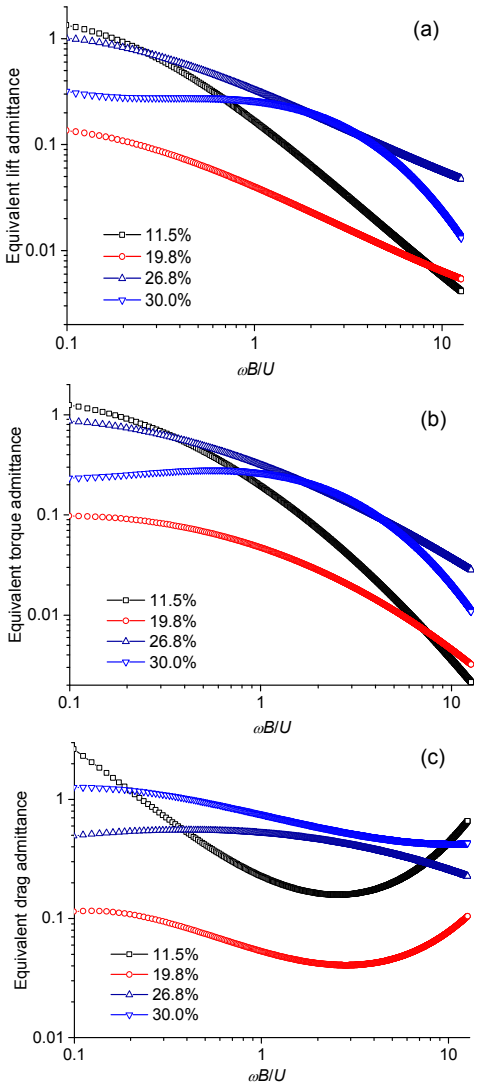

Fig. 10 Comparison of equivalent aerodynamic admittance for various levels of turbulence intensity
(a) Lift force; (b) Torsional moment; (c) Drag force

turbulence about u, v, and w is involved, as in a real atmospheric environment, there are obvious spatial correlations between aerodynamics acting on a streamlined or bluff body along the cross-wind direction. Thus, the admittance function may not be equal to 1.0 even with reduced frequencies close to 0.0, and its value depends on the bluff body configuration and incoming flow parameters (Larose et al., 1998; Matsuda et al., 1999; Li et al., 2018). There is a need for further investigation of these issues. On the other hand, the results presented here indicate the importance of accurately simulating the wind field in a wind tunnel. Furthermore, note that the identified equivalent admittance results do not always present a monotonically decreasing trend with the reduced frequency as indicated in the traditional Sears-like fitted functions (Larose et al., 1998).

4 Identified aerodynamic admittance of bluff bodies

To verify the equivalent aerodynamic admittance, a series of cross sections were chosen (Fig. 11).

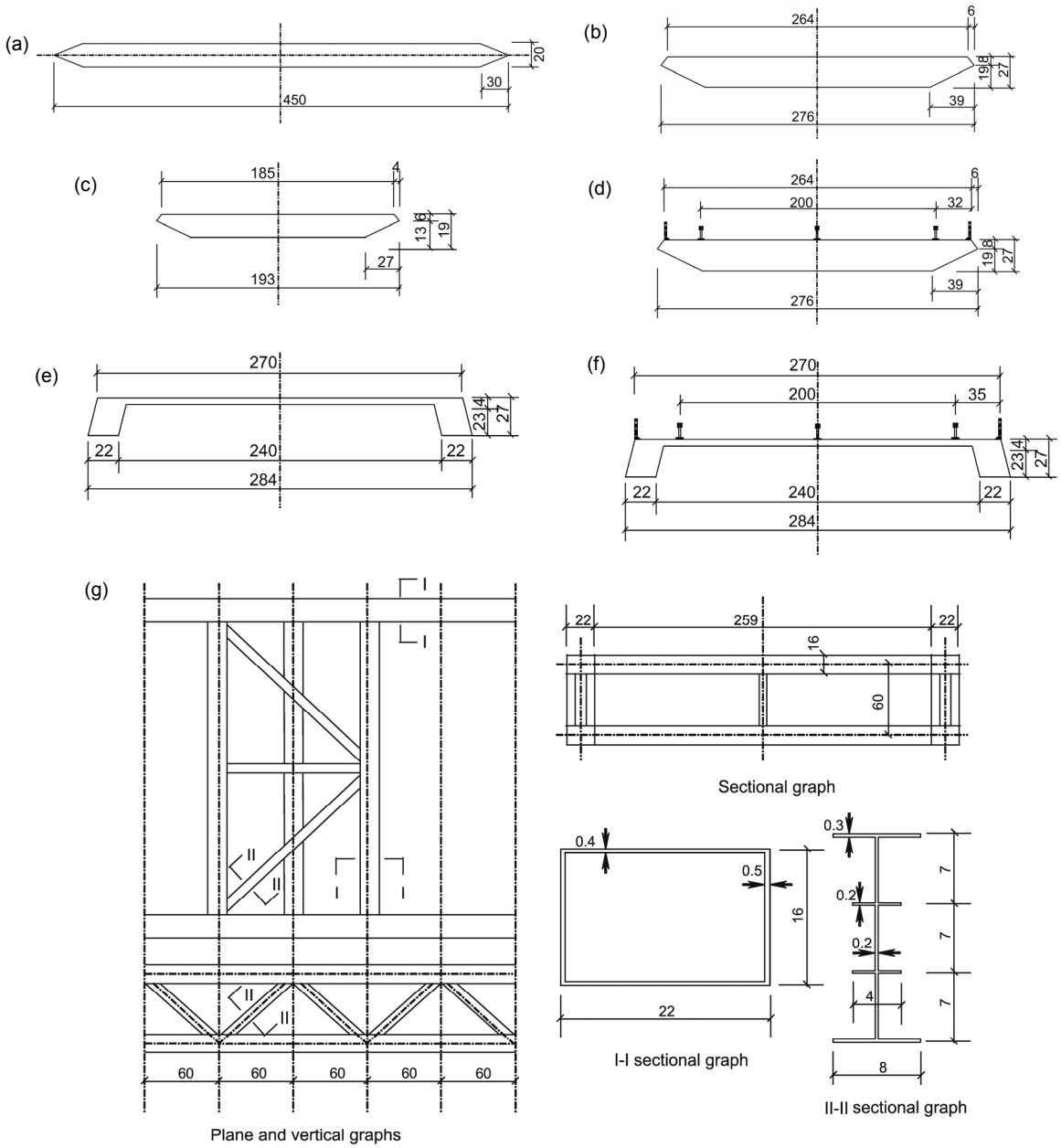

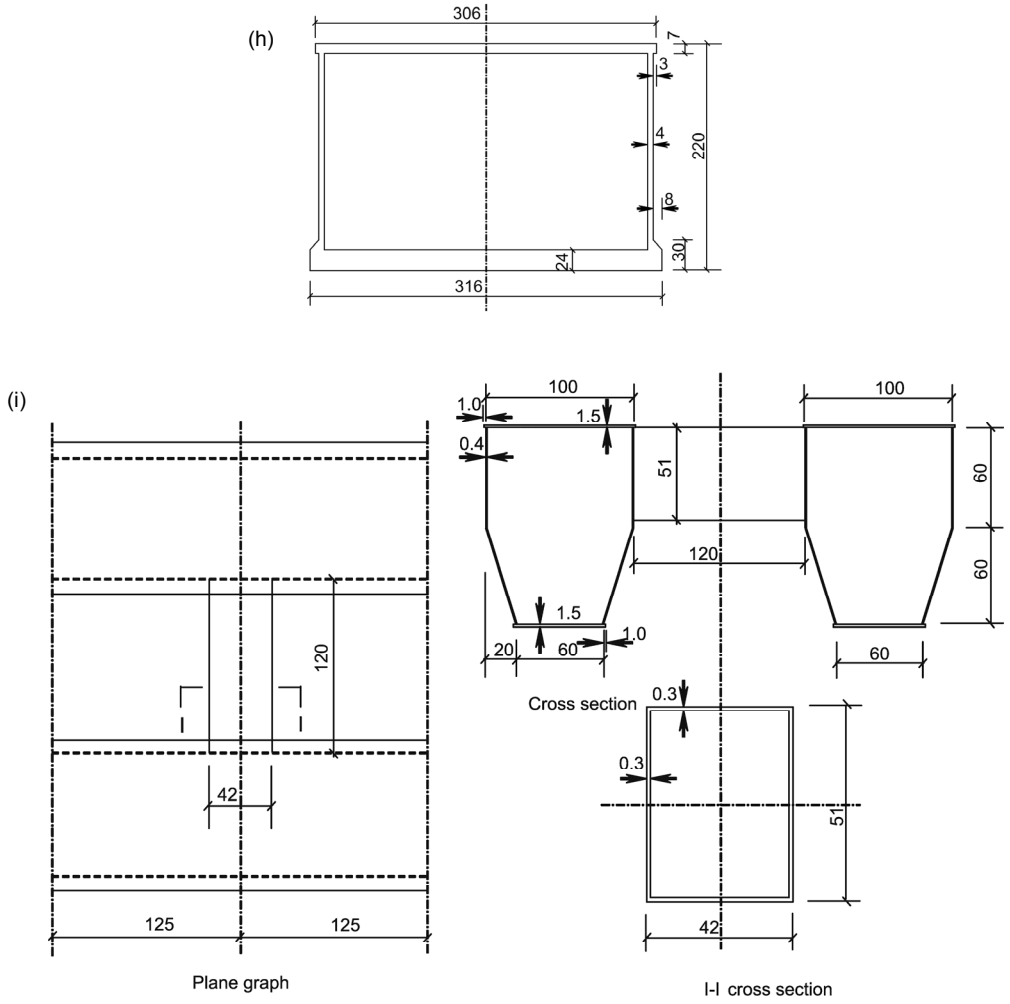

Fig. 11 Typical bridge cross sections (unit: mm)

(a) Plate; (b) Streamlined girder 1; (c) Streamlined girder 2; (d) Streamlined girder+rails; (e) Double-sided girder; (f) Double-sided girder+rails; (g) Trussed girder; (h) Single box; (i) Separated double box

These measurements were made at a mean wind velocity of 5.60 m/s and turbulence intensities of I_u=11.5% and I_w=9.4%. The aerodynamic admittances for various cross sections were quite different. The aerodynamic admittances of some sections were much higher than the quasi-steady value (unit value). The aerodynamic admittances of models with rails were typically larger than those of sections without rails. Fig. 12 and Table 3 present the identified equivalent aerodynamic admittance functions for the cross sections examined. In general, the equivalent aerodynamic admittance of lift force and torsional moment decreased with increasing reduced frequency, whereas for most of the cross sections, this monotonic trend was not necessarily valid for the aerodynamic admittance of the drag force. This result is similar to the observations of Matsuda et al. (1999). For typical bluff deck sections, such as a single box, separated box, and double-sided girder with rails, the equivalent admittance functions present a local hump within the reduced frequency $\omega B/U$ range of 1.0–3.0, resulting from vortex-induced effects.

5 Buffeting response analysis

5.1 Wind tunnel setup

A typical streamlined bridge deck was used to

carry out the buffeting response analysis (Fig. 13). Specifically, the buffeting response calculated based on the identified equivalent aerodynamic admittance was compared to the experimental measurement in the wind tunnel. The model had an aerodynamic configuration similar to that of the force-measured model (Fig. 6). It was 1.70 m long and comprised an aluminum alloy framework with a light and thin wood veneer. The mass of the model was 5.458 kg/m and the mass inertia moment was 0.140 kg·m^2/m. The

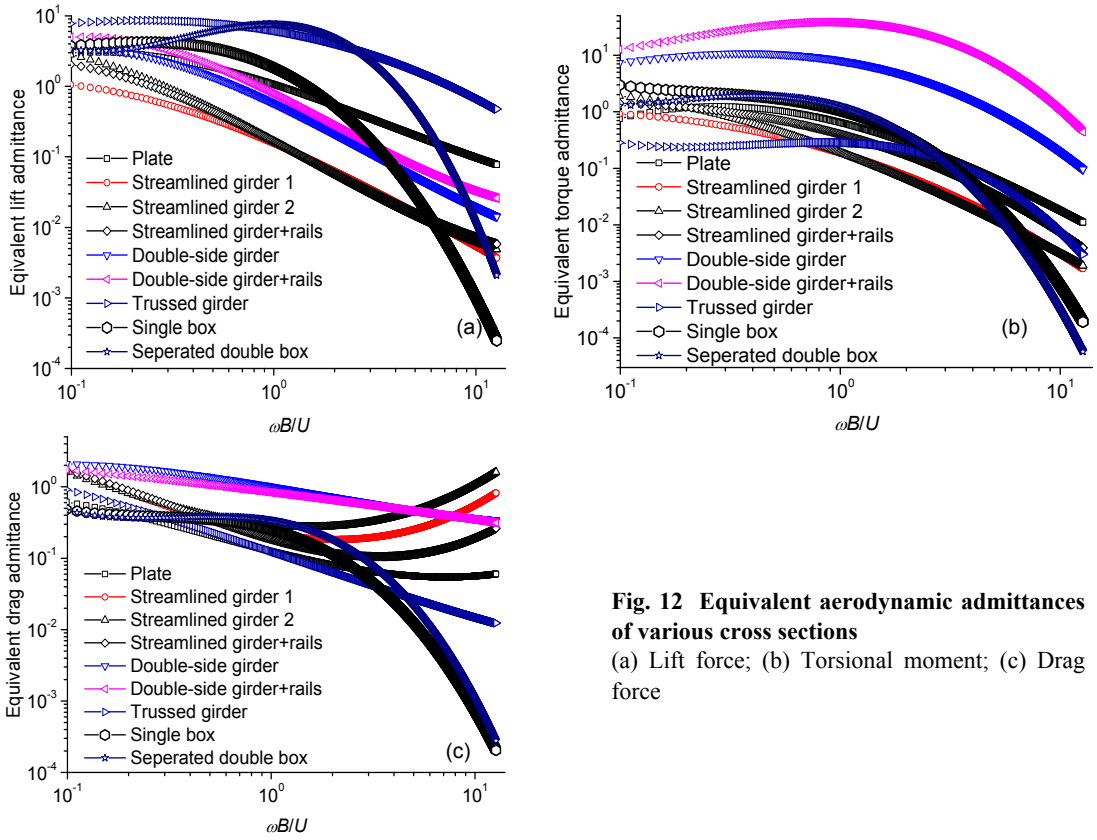

Fig. 12 Equivalent aerodynamic admittances of various cross sections

(a) Lift force; (b) Torsional moment; (c) Drag force

Table 3 Fitted parameters of identified admittance functions of various cross sections

Cross section	Lift admittance				Torsional admittance				Drag admittance			
	α_0	α_1	α_2	α_3	α_0	α_1	α_2	α_3	α_0	α_1	α_2	α_3
Plate	0.02	−0.90	−0.29	0.16	−0.19	−0.96	−0.74	0.15	−0.90	−0.71	0.17	0.19
Streamlined girder 1	−0.80	−1.23	−0.31	0.08	−0.72	−1.18	−0.54	−0.05	−0.65	−0.49	0.64	0.24
Streamlined girder 2	−0.77	−1.55	−0.10	0.22	−0.72	−1.45	−0.39	0.05	−0.53	−0.27	0.65	0.19
Streamlined girder+rails	−0.79	−1.47	−0.13	0.25	−0.40	−1.05	−0.60	−0.09	−0.74	−0.81	0.49	0.33
Double-sided girder	−0.23	−1.36	−0.35	0.24	0.90	−0.61	−0.83	−0.17	0.01	−0.48	−0.06	0.10
Double-sided girder+rails	−0.11	−1.43	−0.28	0.34	1.57	−0.12	−1.01	−0.41	−0.08	−0.35	−0.03	0.00
Trussed girder	0.78	−0.47	−0.42	−0.05	−0.54	−0.10	−0.78	−0.67	−0.90	−0.95	−0.03	0.06
Single box	0.26	−1.32	−1.47	−0.45	0.02	−1.06	−1.32	−0.71	−0.60	−0.76	−1.13	−0.65
Separated double box	0.87	−0.05	−1.58	−1.17	0.09	−1.07	−1.79	−0.72	−0.47	−0.46	−1.18	−0.86

model was designed to ensure that there was no local deformation and vibration during the test.

The test was conducted in the TJ-1 Boundary Layer Wind Tunnel of Tongji University. Fig. 14 shows a schematic drawing of the connection between the measurement segment model and the outside support system. The supporting structure included eight spring systems and two end rods fixed outside the wind tunnel. The model was connected to the support system by a pair of rectangular posts in the wall of the wind tunnel. Both ends of the model were connected by two rigid connecting rods and a horizontal end rod, which was hung by springs. There was a space of only a few centimeters between the end of the model and the tunnel wall. Hence, the wind field could be treated as two dimensional. The model could vibrate in both vertical bending and torsional directions, while the lateral displacement of the model was fixed by four steel wires. The frequencies in vertical bending and torsion were 2.24 and 4.47 Hz, with corresponding damping ratios of 0.49% and 0.52%, respectively. The model buffeting response was captured by laser sensors installed on the end rods. The simulated turbulence intensities in the wind tunnel were I_u=11.5% and I_w=6.5%. The wind-induced displacement of the segment model was measured using MLS-LM10 laser sensors made by the MEW-Matsushita Company and had a measuring range of ±50 mm with a precision of 0.01 mm.

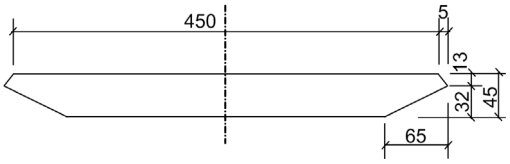

Fig. 13 Cross section of a typical streamlined bridge deck used in the buffeting analysis (unit: mm)

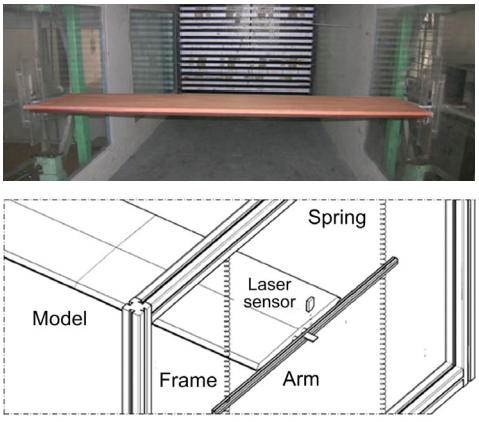

Fig. 14 Schematic of the connection between the measurement segment model and the outside support system

5.2 Buffeting response

The buffeting response was calculated based on Scanlan (1978a, 1978b)'s analysis framework. The steady-state coefficients and self-excited forces employed in the buffeting calculation are expressed in Eqs. (14) and (15), respectively.

$$C_L=\frac{\bar{L}_{\mathrm{b}}}{\frac{1}{2}\rho U^2 Bl}, \tag{14a}$$

$$C_M=\frac{\bar{M}_{\mathrm{b}}}{\frac{1}{2}\rho U^2 B^2 l}, \tag{14b}$$

$$C_D=\frac{\bar{D}_{\mathrm{b}}}{\frac{1}{2}\rho U^2 Bl}, \tag{14c}$$

where $\bar{L}_{\mathrm{b}}$, $\bar{M}_{\mathrm{b}}$, and $\bar{D}_{\mathrm{b}}$ relate to the mean values of the lift force, torsional moment, and drag force, respectively, and l is the length of the model.

$$L_{\mathrm{se}}=\frac{1}{2}\rho U^2(2B)\cdot\left[KH_1^*(K)\frac{\dot{h}}{U}+KH_2^*(K)\frac{B\dot{\alpha}}{U}+K^2H_3^*(K)\alpha+K^2H_4^*(K)\frac{h}{U}\right], \tag{15a}$$

$$M_{\mathrm{se}}=\frac{1}{2}\rho U^2(2B^2)\cdot\left[KA_1^*(K)\frac{\dot{h}}{U}+KA_2^*(K)\frac{B\dot{\alpha}}{U}+K^2A_3^*(K)\alpha+K^2A_4^*(K)\frac{h}{U}\right], \tag{15b}$$

where L_{se} and M_{se} relate to the self-excited lift force and torsional moment; H_i^* and A_i^* (i=1–4) are flutter derivatives; h and α are time related vertical displacements and torsion angle, respectively. The measured steady-state coefficients and flutter derivatives of the streamlined model are shown in Fig. 15. The identified aerodynamic admittance was fitted

using Eq. (13). The fitted parameters of the identified equivalent aerodynamic admittance were α_0=−0.25, α_1=−1.18, α_2=−0.49, α_3=0.60 for the lift force and α_0=−0.19, α_1=−0.97, α_2=−0.74, α_3= 0.15 for the torsional moment (Fig. 16).

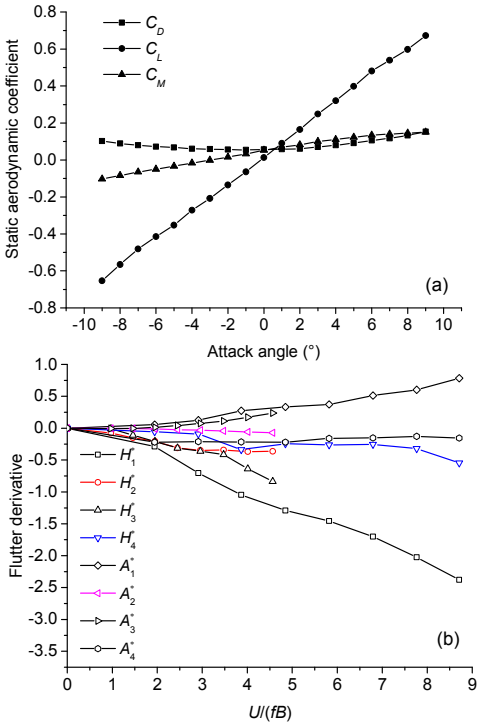

Fig. 15 Steady-state coefficients (a) and flutter derivatives (b) of the streamlined model

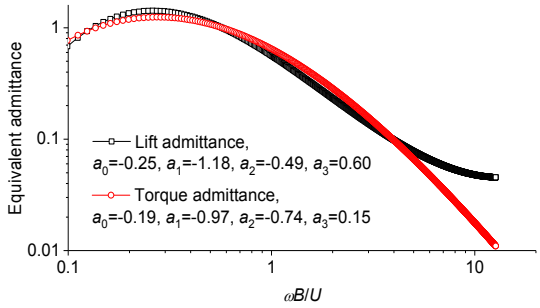

Fig. 16 Identified aerodynamic admittance of the streamlined model

Fig. 17 shows the quasi-steady value (unit), Sears' function, and identified equivalent aerodynamic admittance at various wind velocities. Fig. 18 presents a comparison of the buffeting response measured in the wind tunnel and the calculation results based on various aerodynamic admittance functions. In the numerical calculation, the aerodynamic admittance function was set as the quasi-steady value (unit), the Sears' function or the experimental identification result. The wind spectra used in the numerical simulations were measured in the wind tunnel. Fig. 18 shows that, for the streamlined section, the buffeting response obtained based on both Sears' function and the identified aerodynamic admittance compared well with the measured results, whereas the results based on quasi-steady theory were very conservative.

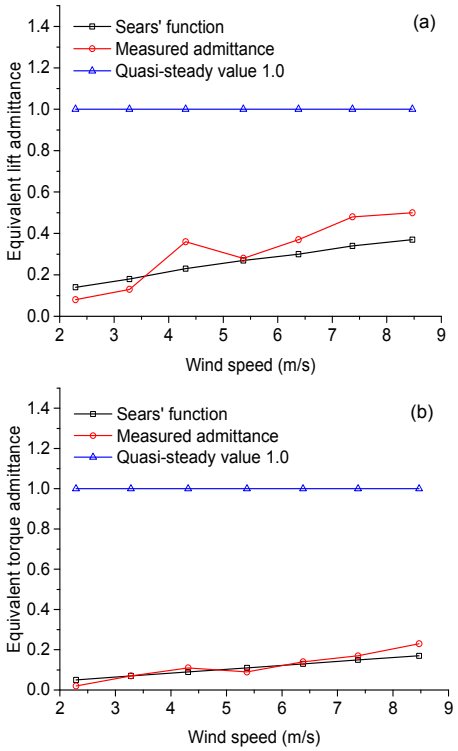

Fig. 17 Aerodynamic admittance based on the quasi-steady theory, Sears' function, and identification results at various wind velocities

(a) Lift force; (b) Torsional moment

6 Sensitivity analysis of buffeting response

The sensitivity of the buffeting response to various parameters associated with wind, aerodynamics, and structural attributes was investigated based on the following sensitivity index (Haldar and Mahadevan, 2000)

$$\gamma_{Yi}(x_i)=\frac{\Delta_{Yi}(x_i)}{\left[\sum_{i=1}^{N}\Delta_{Yi}^2(x_i)\right]^{0.5}}, \tag{16}$$

$$\Delta_{Yi}(x_i)=\frac{Y(x_i+\sigma_i)-Y(x_i-\sigma_i)}{2.0}, \tag{17}$$

where γ is the sensitivity index; N is the number of uncertain parameters x_i; Δ is a mathematical increment symbol; Y is the vertical or torsional buffeting response; σ_i is the root mean square (RMS) value of the uncertain parameters. A total of 33 parameters were considered in the investigation: mean wind velocity U, model width D, lumped mass M, inertial moment I, vertical damping ratio ξ_h, torsional damping ratio ξ_α, vertical natural frequency ω_h, torsional natural frequency ω_α, drag coefficient C_D, lift coefficient C_L, derivative of lift coefficient C_L', torsional coefficient C_M, derivative of torsional coefficient C_M', longitudinal wind spectra $S_{uu}(\omega_h)$ and $S_{uu}(\omega_\alpha)$, vertical wind spectra $S_{ww}(\omega_h)$ and $S_{ww}(\omega_\alpha)$, aerodynamic admittances of lift force $\chi_{Lu}(\omega_h)$, $\chi_{Lu}(\omega_\alpha)$, $\chi_{Lw}(\omega_h)$, and $\chi_{Lw}(\omega_\alpha)$, aerodynamic admittances of torsional force $\chi_{Mu}(\omega_h)$, $\chi_{Mu}(\omega_\alpha)$, $\chi_{Mw}(\omega_h)$, and $\chi_{Mw}(\omega_\alpha)$, and flutter derivatives H_1^*, H_2^*, H_3^*, H_4^*, A_1^*, A_2^*, A_3^*, and A_4^*. The RMS value was determined from the statistics derived from wind tunnel tests. Specifically, four typical values for the coefficient of variance were used in the sensitivity analysis, namely 2%, 5%, 10%, and 15%. The buffeting response was calculated based on two different approaches. Approach 1 (M1) assumed $\chi_{Fu}(\omega)=\chi_{Fw}(\omega)$, while approach 2 (M2) considered different contributions from the longitudinal and vertical fluctuations (e.g. different values of $\chi_{Fu}(\omega)$ and $\chi_{Fw}(\omega)$ were employed based on the proposed identification scheme).

Figs. 19 and 20 present the results from sensitivity analysis of the vertical and torsional buffeting responses to the 33 parameters. Similar buffeting response sensitivity results were obtained using the two approaches. In general, the buffeting response was very sensitive to the mean wind velocity, natural frequency, and derivatives of steady-state coefficients ($0.40\leq\gamma\leq0.60$). Furthermore, it was much more sensitive to the aerodynamic admittance functions ($0.16\leq\gamma\leq0.39$) than to the flutter derivatives ($0.11\leq\gamma\leq0.20$), which highlights the importance of accurate identification of aerodynamic admittance. Fig. 21 gives a comparison of the sensitivity analysis results of buffeting response based on M1 and M2. For M1, the buffeting lift force was not sensitive to the steady-state lift coefficient, but was very sensitive to its derivatives. On the other hand, the M2 buffeting lift force showed similar sensitivity to both the steady-state lift coefficient and its derivative. M2 can effectively consider the contribution of the longitudinal fluctuation, which relates to the steady-state lift coefficient, to the buffeting response.

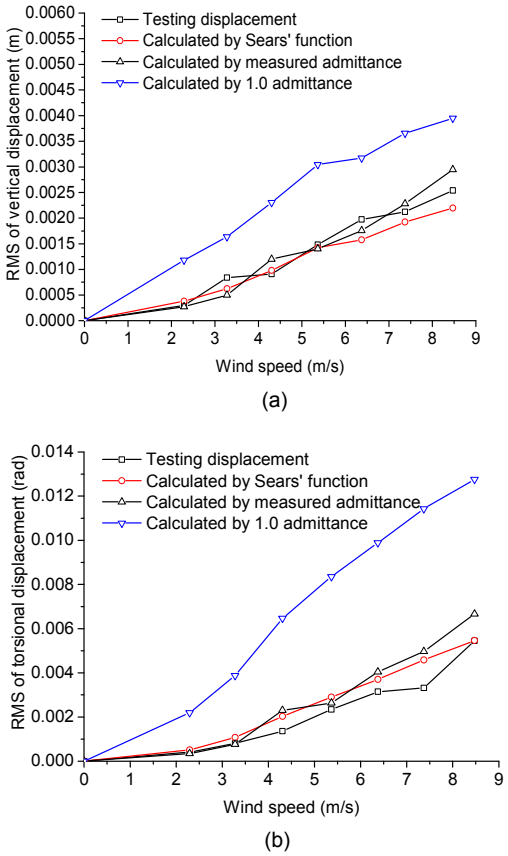

Fig. 18 Comparison of the buffeting response measured in the wind tunnel and the calculation results based on various aerodynamic admittance functions
(a) Vertical displacement; (b) Torsional displacement

7 Concluding remarks

A framework is proposed to identify a comprehensive set of aerodynamic admittance functions. The contributions of the cross-spectra between longitudinal and vertical fluctuations, and between the incident turbulence and the gust-induced forces, are considered during the identification procedure. To promote convenient application of the identified

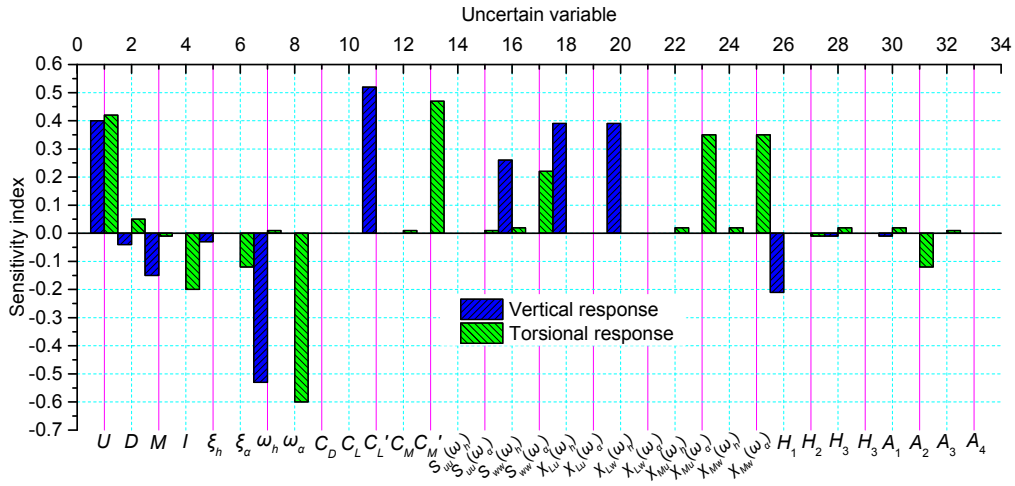

Fig. 19 Buffeting response sensitivity of a streamlined model based on M1

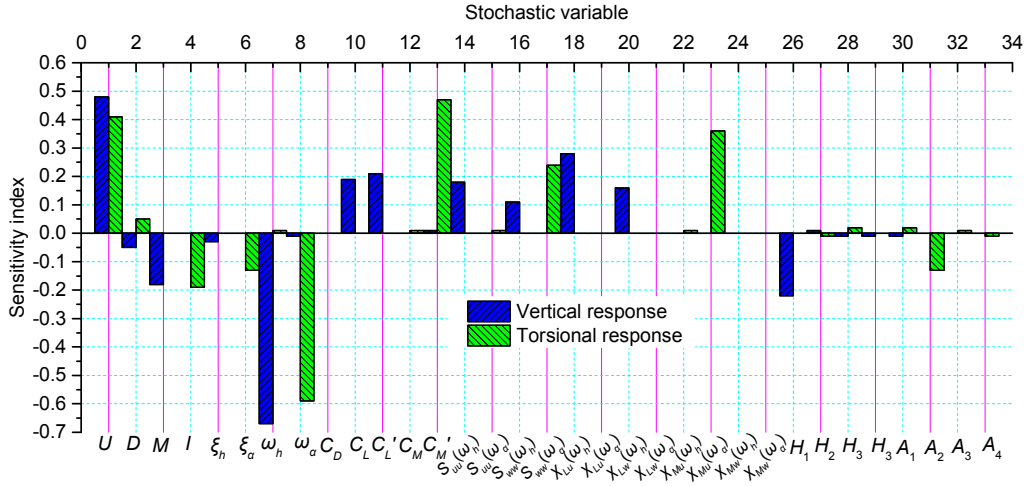

Fig. 20 Buffeting response sensitivity of a streamlined model based on M2

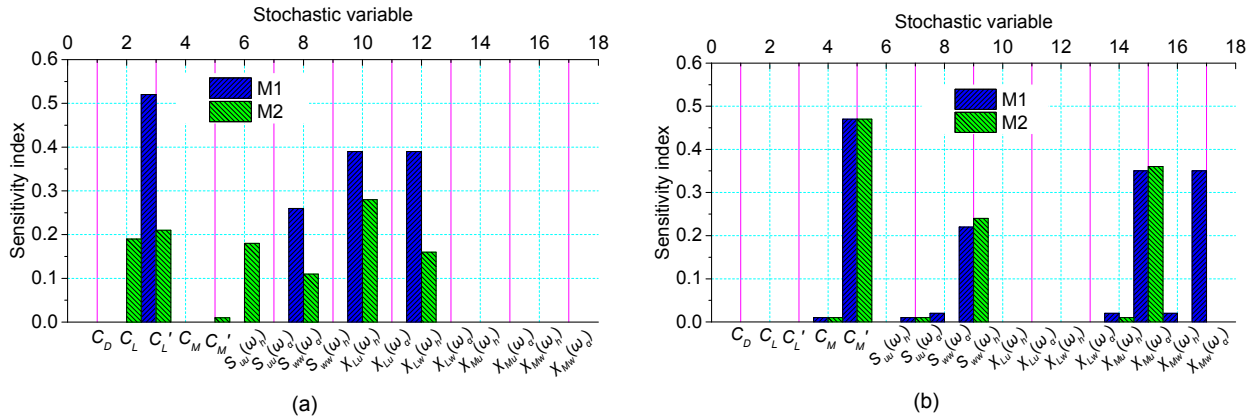

Fig. 21 Comparison of sensitivity analysis based on M1 and M2
(a) Sensitivity of vertical response; (b) Sensitivity of torsional response

aerodynamic admittance functions in engineering practice, equivalent aerodynamic admittance functions for the lift force, torsional moment, and drag force are introduced. The identified equivalent aerodynamic admittance functions were systematically validated through a numerical study and found to bear high fidelity. In addition, the identified equivalent aerodynamic admittance functions of a streamlined bridge deck in a wind tunnel showed a good agreement with the results of a stochastic subspace identification technique, which further demonstrated the effectiveness of the proposed identification framework. Furthermore, the aerodynamic admittance was identified in the wind tunnel for a set of streamlined and bluff cross sections. The aerodynamic admittance of some cross sections was higher than those based on quasi-steady theory (unit). In general, the identified equivalent aerodynamic admittances of the lift force and torsional moment decreased with the reduced frequency. However, for most of the bluff cross sections studied, this monotonic property did not necessarily exist for the aerodynamic admittance of the drag force. The buffeting response was calculated based on the aerodynamic admittance function of the quasi-steady valued (unit), Sears' function, and the experimentally identified functions, and compared to the measured results in the wind tunnel. The results suggest that, for a streamlined cross section, the use of either Sears' function or the equivalent aerodynamic admittance function is reasonable, while the buffeting response obtained with quasi-steady theory is overly conservative. Finally, the sensitivity analysis indicated that the buffeting response is very sensitive to the mean wind velocity, aerodynamic admittance functions, steady-state coefficients and their derivatives, and flutter derivatives.

Contributors

Lin ZHAO wrote the manuscript. Xi XIE conducted the wind tunnel tests. Teng WU revised and polished this paper. Shao-peng LI and Zhi-peng LI carried out the buffeting analysis. Yao-jun GE and Ahsan KAREEM gave the concepts and modification of this paper.

Conflict of interest

Lin ZHAO, Xi XIE, Teng WU, Shao-peng LI, Zhi-peng LI, Yao-jun GE, and Ahsan KAREEM declare that they have no conflict of interest.

References

Cao BC, Sarkar PP, 2013. Time-domain aeroelastic loads and response of flexible bridges in gusty wind: prediction and experimental validation. *Journal of Engineering Mechanics*, 139(3):359-366. https://doi.org/10.1061/(ASCE)EM.1943-7889.0000502

Chen XZ, Kareem A, 2001. Nonlinear response analysis of long-span bridges under turbulent winds. *Journal of Wind Engineering and Industrial Aerodynamics*, 89(14-15): 1335-1350. https://doi.org/10.1016/S0167-6105(01)00147-7

Davenport AG, 1962. Buffeting of a suspension bridge by storm winds. *Journal of the Structural Division*, 88(3): 233-270.

Deodatis G, 1996. Simulation of ergodic multivariate stochastic processes. *Journal of Engineering Mechanics*, 122(8): 778-787. https://doi.org/10.1061/(asce)0733-9399(1996)122:8(778)

Diana G, Bruni S, Cigada A, et al., 2002. Complex aerodynamic admittance function role in buffeting response of a bridge deck. *Journal of Wind Engineering and Industrial Aerodynamics*, 90(12-15):2057-2072. https://doi.org/10.1016/S0167-6105(02)00321-5

Ge YJ, Zhao L, 2014. Wind-excited stochastic vibration of long-span bridge considering wind field parameters during typhoon landfall. *Wind and Structures*, 19(4):421-441. https://doi.org/10.12989/was.2014.19.4.421

Gu M, Qin XR, 2004. Direct identification of flutter derivatives and aerodynamic admittances of bridge decks. *Engineering Structures*, 26(14):2161-2172. https://doi.org/10.1016/j.engstruct.2004.07.015

Haan Jr FL, Wu T, Kareem A, 2016. Correlation structures of pressure field and integrated forces on oscillating prism in turbulent flows. *Journal of Engineering Mechanics*, 142(5):04016017. https://doi.org/10.1061/(ASCE)EM.1943-7889.0001058

Haldar A, Mahadevan S, 2000. Reliability Assessment Using Stochastic Finite Element Analysis. John Wiley & Sons, New York, USA.

Hatanaka A, Tanaka H, 2002. New estimation method of aerodynamic admittance function. *Journal of Wind Engineering and Industrial Aerodynamics*, 9(12-15):2073-2086. https://doi.org/10.1016/S0167-6105(02)00324-0

Horlock JH, 1968. Fluctuating lift forces on aerofoils moving through transverse and chordwise gusts. *Journal of Basic Engineering*, 90(4):494-500. https://doi.org/10.1115/1.3605173

Jain A, Jones NP, Scanlan RH, 1996. Coupled flutter and buffeting analysis of long-span bridges. *Journal of Structural Engineering*, 122(7):716-725. https://doi.org/10.1061/(asce)0733-9445(1996)122:7(716)

Jancauskas ED, Melbourne WH, 1986. The aerodynamic admittance of two-dimensional rectangular section cylinders in smooth flow. *Journal of Wind Engineering and Industrial Aerodynamics*, 23:395-408. https://doi.org/10.1016/0167-6105(86)90057-7

Lamson P, 1966. Measurements of Lift Fluctuations Due to Turbulence. PhD Thesis, California Institute of Technology, Pasadena, USA.

Larose GL, 2003. The spatial distribution of unsteady loading due to gusts on bridge decks. *Journal of Wind Engineering and Industrial Aerodynamics*, 91(12-15):1431-1443. https://doi.org/10.1016/j.jweia.2003.09.008

Larose GL, Mann J, 1998. Gust loading on streamlined bridge decks. *Journal of Fluids and Structures*, 12(5):511-536. https://doi.org/10.1006/jfls.1998.0161

Larose GL, Tanaka H, Gimsing NJ, et al., 1998. Direct measurements of buffeting wind forces on bridge decks. *Journal of Wind Engineering and Industrial Aerodynamics*, 74-76:809-818. https://doi.org/10.1016/S0167-6105(98)00073-7

Li MS, Yang Y, Li M, et al., 2018. Direct measurement of the Sears function in turbulent flow. *Journal of Fluid Mechanics*, 847:768-785. https://doi.org/10.1017/jfm.2018.351

Liepmann HW, 1952. On the application of statistical concepts to the buffeting problem. *Journal of the Aeronautical Sciences*, 19(12):793-800. https://doi.org/10.2514/8.2491

Ma TT, Zhao L, Cao SY, et al., 2013. Investigations of aerodynamic effects on streamlined box girder using two-dimensional actively-controlled oncoming flow. *Journal of Wind Engineering and Industrial Aerodynamics*, 122:118-129. https://doi.org/10.1016/j.jweia.2013.07.011

Matsuda K, Hikami Y, Fujiwara T, et al., 1999. Aerodynamic admittance and the 'strip theory' for horizontal buffeting forces on a bridge deck. *Journal of Wind Engineering and Industrial Aerodynamics*, 83(1-3):337-346. https://doi.org/10.1016/S0167-6105(99)00083-5

Matsuda K, Cooper KR, Tanaka H, et al., 2001. An investigation of Reynolds number effects on the steady and unsteady aerodynamic forces on a 1:10 scale bridge deck section model. *Journal of Wind Engineering and Industrial Aerodynamics*, 89(7-8):619-632. https://doi.org/10.1016/S0167-6105(01)00062-9

Nicholas M, Ogden PM, Erskine FT, 1998. Improved empirical descriptions for acoustic surface backscatter in the ocean. *IEEE Journal of Oceanic Engineering*, 23(2):81-95. https://doi.org/10.1109/48.664088

Pan T, 2013. Non-steady Aerodynamic Force Models of Bridge and Analysis on Wind-induced Vibration. PhD Thesis, Tongji University, Shanghai, China (in Chinese).

Sankaran R, Jancauskas ED, 1992. Direct measurement of the aerodynamic admittance of two-dimensional rectangular cylinders in smooth and turbulent flows. *Journal of Wind Engineering and Industrial Aerodynamics*, 41(1-3):601-611. https://doi.org/10.1016/0167-6105(92)90469-Q

Scanlan RH, 1978a. The action of flexible bridges under wind, I: flutter theory. *Journal of Sound and Vibration*, 60(2):187-199. https://doi.org/10.1016/S0022-460X(78)80028-5

Scanlan RH, 1978b. The action of flexible bridges under wind, II: buffeting theory. *Journal of Sound and Vibration*, 60(2):201-211. https://doi.org/10.1016/S0022-460X(78)80029-7

Scanlan RH, Jones NP, 1999. A form of aerodynamic admittance for use in bridge aeroelastic analysis. *Journal of Fluids and Structures*, 13(7-8):1017-1027. https://doi.org/10.1006/jfls.1999.0243

Walshe DE, Wyatt TA, 1983. Measurement and application of the aerodynamic admittance function for a box-girder bridge. *Journal of Wind Engineering and Industrial Aerodynamics*, 14(1-3):211-222. https://doi.org/10.1016/0167-6105(83)90024-7

Wu T, Kareem A, 2014. Revisiting convolution scheme in bridge aerodynamics: comparison of step and impulse response functions. *Journal of Engineering Mechanics*, 140(5):04014008. https://doi.org/10.1061/(ASCE)EM.1943-7889.0000709

Xu K, Zhao L, Cao SY, et al., 2014. Investigation of spatial coherences of aerodynamic loads on a streamlined bridge deck in an actively-controlled wind tunnel. *Advances in Structural Engineering*, 17(1):53-65. https://doi.org/10.1260/1369-4332.17.1.53

中文概要

题　目： 回顾与讨论气动导纳函数

目　的： 提出一种识别桥面气动导纳函数的理论框架并验证其合理性。

方　法： 1. 提出一种考虑来流脉动风和气动力全部交叉分量贡献的全分量导纳函数的识别算法。2. 利用风洞试验与数值分析结合的方法，对一组流线型和钝体断面的气动导纳进行验证。3. 对一桥梁断面进行抖振响应分析，验证其等效气动导纳。

结　论： 1. 通过数值计算，系统地验证了本文所提出的等效气动导纳函数具有较高的保真度。2. 风洞中流线型断面的等效气动导纳函数的辨识结果与随机子空间辨识方法的结果吻合良好。3. 通过对一组流线型和钝体断面进行气动导纳识别表明，某些断面的气动导纳高于基于准定常理论的所得值。4. 根据准定常理论下的气动导纳函数、Sears 函数和实验验证的函数计算抖振响应并与风洞试验结果进行比较发现，对于流线型断面，采用 Sears 函数或等效气动导纳函数都是合理的，而用准定常理论得到的抖振响应则过于保守。5. 灵敏度分析表明，抖振响应对平均风速、气动导纳函数、静风力系数及其导数和颤振导数等参数非常敏感。

关键词： 气动导纳函数；桥梁断面；抖振分析；风洞试验；灵敏度分析